The above does not agree with the assertion that "with increase in blow energy the effect of instrument geometry on efficiency of rock breakup decreases significantly..." [7, p. 29]. The numerical experiments performed show that with increase in blow energy one can in principle achieve destruction of the block material with every blow.

LITERATURE CITED

1. S. K. Godunov, A. V. Zabrodin, M. Ya. Ivanov, et al., Numerical Solution of Multidimensional Gas Dynamics Problems [in Russian], Nauka, Moscow (1976).
2. G. V. Ivanov, "Construction of solution methods for the planar dynamic problem of elasticity theory by approximation by linear polynomials," in: Dynamics of Continuous Media, Collected Works, Academy of Sciences of the USSR, Siberian Branch, Hydrodynamics Institute [in Russian], No. 37 (1978).
3. Yu. M. Volchkov, G. V. Ivanov, and V. D. Kurguzov, "Algorithm for splitting the planar dynamic problem of elastic deformation with consideration of coarse scale destruction," in: Dynamics of Continuous Media, Collected Works, Academy of Sciences of the USSR, Siberian Branch, Hydrodynamics Institute [in Russian], No. 48 (1983).
4. I. O. Bogul'skii, "Increasing accuracy of the solution of planar dynamic elasticity problems with approximation by linear polynomials," Dep. VINITI 1/3/86, No. 65-86 (1986).
5. S. N. Zhurkov, The problem of strength of solid bodies," Vestn. Akad. Nauk SSSR, No. 11 (1957).
6. V. A. Stepanov, N. N. Peschanskaya, and V. V. Shpeizman, Strength and Relaxation Phenomena in Solids [in Russian], Leningrad, Nauka (1984).
7. B. V. Voitsekhovskii, L. A. Mitin, and F. F. Voitsekhovskaya, "Effectiveness of high energy impact for destruction of large rock," FTPRPI, No. 4 (1973).

ANALYSIS OF CREEP IN A RECTANGULAR PLATE WITH A CIRCULAR ORIFICE UNDER TENSION

V. N. Solodovnikov

UDC 539.376

A finite element solution of the problem is offered using the theory of strengthening type creep. Because of creep the stress concentration at the edge of the orifice is reduced, and displacement as a function of reduced time increases at an almost constant rate. Moiré type displacement isoline patterns are presented.

Fundamental Equations. Expressions for the deformations in terms of displacements, the equilibrium equation, and relationships between stresses and deformations in the plane stressed state are taken in the form [1, 2]

$$e_{11} = u_{1,1},\ e_{22} = u_{2,2},\ 2e_{12} = u_{1,2} + u_{2,1},$$
$$\sigma_{11,1} + \sigma_{12,2} = 0,\ \sigma_{12,1} + \sigma_{22,2} = 0,$$
$$e_{11} = E^{-1}(\sigma_{11} - \nu\sigma_{22}) + \rho_{11},\ e_{22} = E^{-1}(\sigma_{22} - \nu\sigma_{11}) + \rho_{22},$$
$$e_{12} = (1 + \nu)E^{-1}\sigma_{12} + \rho_{12}.$$

Here E is Young's modulus, ν is the Poisson coefficient, u_i are the displacements; e_{ij}, the deformations; σ_{ij}, the stresses; ρ_{ij} are the creep deformations (i, j = 1, 2) in the Cartesian coordinate system x_1, x_2; the subscripts 1 and 2 following the comma indicate partial differentiation with respect to x_1 and x_2, respectively.

In contrast to [3-7], to calculate plate creep we will use the strengthening type creep theory of [2, 8]. In the uniaxially stressed state the creep deformation ρ and the stress σ as a function of time t are interrelated in this theory by an expression

$$\rho^k d\rho/dt = a\sigma^n, \tag{1}$$

Novosibirsk. Translated from Zhurnal Prikladnoi Mekhaniki i Tekhnicheskoi Fiziki, No. 2, pp. 153-157, March-April, 1991. Original article submitted May 22, 1989; revision submitted November 3, 1989.

0021-8944/91/3202-0284$12.50

where k, n, a are positive constants of the material. At the initial moment t = 0 there is a singularity: ρ = 0, the creep deformation rate dρ/dt increases without limit. To eliminate this singularity we transform to a new time variable, the reduced time [8]

$$\tau = [a(k+1)t]^m, \quad m = 1/(k+1). \tag{2}$$

From Eqs. (1) and (2) we obtain

$$\rho^k \dot{\rho} = \tau^k \sigma^n, \quad \dot{\rho} = \sigma^n \left[(k+1)\,\tau^{-(k+1)} \int_0^\tau \sigma^n \tau^k \, d\tau \right]^{m-1}. \tag{3}$$

The dot above a quantity indicates differentiation with respect to τ. At τ = 0 the derivative $\dot{\rho}$ has a finite value σ^{mn}. For brevity we will refer to τ as time below, while the derivatives with respect to τ will be called the rates of the functions in question.

Generalizing Eq. (3) to a planar stressed state, we write the equation

$$\dot{\rho}_{11} = \lambda(2\sigma_{11} - \sigma_{22}), \quad \dot{\rho}_{22} = \lambda(2\sigma_{22} - \sigma_{11}), \quad \dot{\rho}_{12} = 3\lambda\sigma_{12},$$
$$\lambda = (1/2)\, S^{n-1} \left[(k+1)\,\tau^{-(k+1)} \int_0^\tau S^n \tau^k \, d\tau \right]^{m-1}, \quad S = \left(\sigma_{11}^2 - \sigma_{11}\sigma_{22} + \sigma_{22}^2 + 3\sigma_{12}^2\right)^{1/2} \tag{4}$$

(where S is the stress intensity).

We introduce the functional

$$\Phi = \int_\Omega \int \frac{E}{2(1-\nu^2)} \{ e_{11}^2 + 2\nu e_{11} e_{22} + e_{22}^2 + 2(1-\nu) e_{12}^2 -$$
$$- 2[(\rho_{11} + \nu\rho_{22}) e_{11} + (\rho_{22} + \nu\rho_{11}) e_{22} + 2(1-\nu)\rho_{12} e_{12}] \} \, dx_1 \, dx_2 - \int_\Gamma [p(u_1 l_2 - u_2 l_1) + q(u_1 l_1 + u_2 l_2)] \, dl. \tag{5}$$

Integration is carried out over the region Ω, occupied by the plate, and along its contour Γ. In the given functional the displacements are varied. The deformations e_{11}, e_{22}, e_{12} are expressed in terms of displacements. The creep deformations ρ_{11}, ρ_{22}, ρ_{12}, the normal and tangent stresses p, q on the contour Γ are defined by the expressions (where l_1, l_2 are components of the unit vector tangent to Γ)

$$p = \sigma_{11} l_2^2 - 2\sigma_{12} l_1 l_2 + \sigma_{22} l_1^2, \quad q = (\sigma_{11} - \sigma_{22})\, l_1 l_2 + \sigma_{12}(l_2^2 - l_1^2),$$
$$l_1 = dx_1/dl, \quad l_2 = dx_2/dl, \quad dl = [(dx_1)^2 + (dx_2)^2]^{1/2},$$

are fixed during variation of the functional Φ.

From the condition of steady state of Φ there follow equilibrium equations, formulated in terms of displacements, while the expressions for p and q on Γ are expressed in terms of displacements. We will use the given functional to formulate the finite element equations.

Formulation of the Problem. A rectangular plate with central circular orifice is placed under tension under creep conditions by a constant load P, uniformly distributed along its short edges. In view of the symmetry involved, the solutions will be found for the quarter of the plate depicted in Fig. 1, where the plate dimensions are given with reference to the orifice radius R, and the plate is shown divided into finite elements.

We have the following segments of the contour for the quarter plate and boundary conditions theorem for any τ (see Fig. 1): 1) $R \leqslant x_1 \leqslant L$, $x_2 = 0$, $u_2 = 0$, $\sigma_{12} = 0$; 2) $x_1 = 0$, $R \leqslant x_2 \leqslant H$, $u_1 = 0$, $\sigma_{12} = 0$; 3) $0 \leqslant x_1 \leqslant L$, $x_2 = H$, $\sigma_{22} = \sigma_{12} = 0$; 4) $x_1 = L$, $0 \leqslant x_2 \leqslant H$, $\sigma_{11} = P$, $\sigma_{12} = 0$; 5) $x_1^2 + x_2^2 = R^2$, p = q = 0.

Finite element formulation of the problem. We will use four-sided nine-node isoparametric Lagrangian elements [9]. In all we have 105 elements with 900 unknown variables – the displacement components at the corners of the elements (Fig. 1).

From the condition of steady state of Φ, Eq. (5), considering the specified boundary conditions, we obtain finite element equations in the displacements at the element nodes. To calculate the integrals over the area of each element we use a three-point quadratic Gaussian formula. On the boundaries between the elements the condition of stress continuity is satisfied, and at each node the sum of all applied generalized forces, defined from the principle of possible displacements, is taken equal to zero.

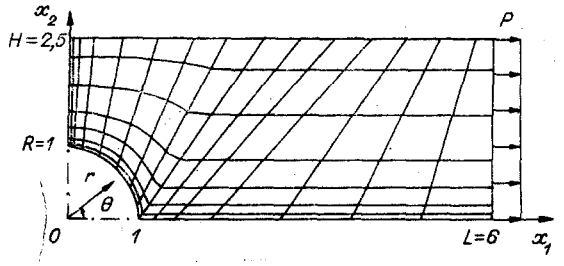

Fig. 1

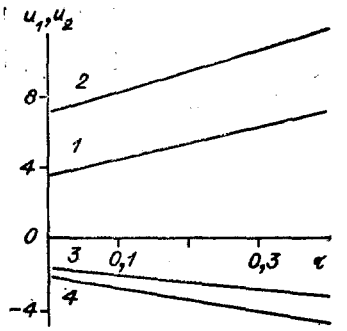

Fig. 2

Differentiating the finite element equations obtained with respect to τ, we arrive at a system of equations for calculation of the displacement rates. The coefficient matrix A for the unknown displacement rates in the equations coincides with the global rigidity and elasticity matrix. The system was solved by the compact Gaussian elimination method with consideration of the sysmmetry and ribbonlike nature of the matrix A [9, 10], with the latter being reduced to triangular form only once in the first solution of the elasticity problem.

Algorithm for Computation over Time. We will determine the initial elastic state of the plate at $\tau = 0$. We then divide τ into small intervals (steps).

In each step from τ to $\tau + \Delta\tau$ for any unknown function v (displacements of element nodes and stresses in the nodes in the expressions for integration over the region Ω) we use the values of v_τ to calculate the rates $\dot{v}_\tau$ at the beginning of the step [we denote function values by a time index (τ or $\tau + \Delta\tau$) to which they refer]. Then, using the values of the stresses $v^*_{\tau+\Delta\tau}$, obtainable by Euler's expression

$$v^*_{\tau+\Delta\tau} = v_\tau + \Delta\tau \dot{v}_\tau,$$

we find the displacement and stress rates $\dot{v}^*_{\tau+\Delta\tau}$, and then use the latter to find the final values of the unknowns at the end of the step $v_{\tau+\Delta\tau} = v_\tau + (\Delta\tau/2)(\dot{v}_\tau + \dot{v}^*_{\tau+\Delta\tau})$. As a result the stressed and deformed state of the plate at the end of the step is fully defined.

We specify the increments in the values of the integrals in the expressions for creep deformation rates (4) $I(\tau) = \int_0^\tau S^n \tau^h \, d\tau$ in the step from τ to $\tau + \Delta$ with the expressions

$$I_{\tau+\Delta\tau} = I_\tau + m(\tau + \Delta\tau)^{h+1}\left[\gamma S^n_\tau + (m+1)^{-1}(1 - m\gamma\tau/\Delta\tau)\left(S^n_{\tau+\Delta\tau} - S^n_\tau\right)\right], \qquad \gamma = 1 - [\tau/(\tau + \Delta\tau)]^{h+1},$$

which are obtained by approximating the function S^n in the step by a linear polynomial. In the final state after complete instantaneous unloading the stresses and displacements are equal to the differences of their values before loading and in the initial elastic state.

Calculation Results. We take the Poisson coefficient $\nu = 0.3$, and the constants in the creep law $n = 9$, $k = 2$, so that $m = 1/3$. We introduce the dimensionless quantities

$$x'_i = x_i/R, \; u'_i = Eu_i/(PR), \; \tau' = \tau E P^{mn-1}, \qquad e'_{ij} = Ee_{ij}/P, \; \sigma'_{ij} = \sigma_{ij}/P \;\; (i, j = 1, 2).$$

In these quantities the solution does not depend on the constants a, E, P, R. In the text below we will omit the primes in the symbols for the dimensionless quantities.

In the interval $0 \leqslant \tau \leqslant T = 0.4$ we specify a sequence of 20 steps: $\Delta\tau = 0.001$, 0.002, 0.004, 0.008, 0.015, 0.02, 0.025,...,0.025.† At $\tau = T$ the stress rates become less than the specified small quantity, the stresses and elastic deformations become practically constant, while the creep deformations continue to grow. At this moment complete instantaneous unloading is carried out. We will note that the actual time t corresponding to $\tau = T$ depends on P, a, E.

The displacements as a function of τ continue to grow at an almost constant rate [according to Eq. (2), the dependence of displacements on t is nonlinear]. The digits 1-4 of Fig. 2 denote graphs of displacements u_1 at points with coordinates (R, 0) and (L, 0) and u_2 at points (0, R) and (0, H) as functions of τ.

†As in Russian original – Editor

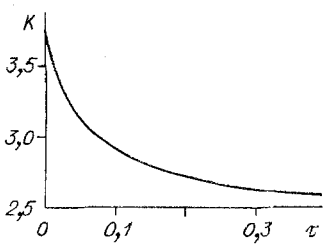

Fig. 3

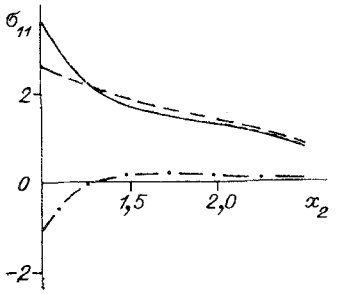

Fig. 4

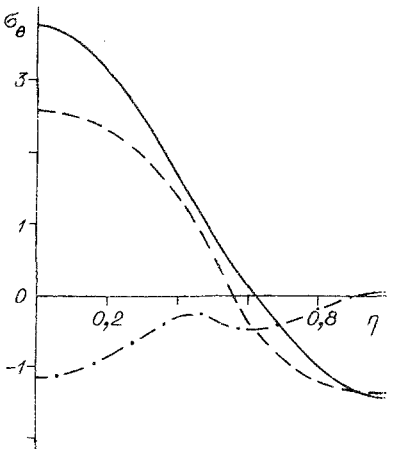

Fig. 5

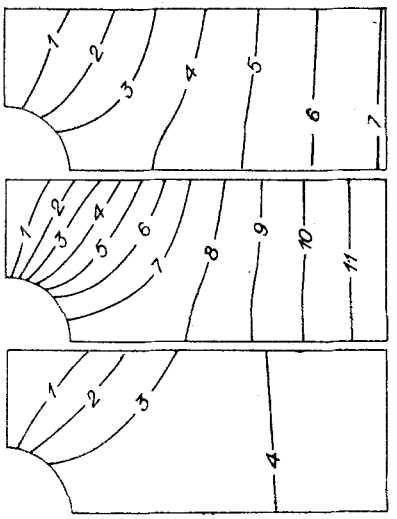

Fig. 6

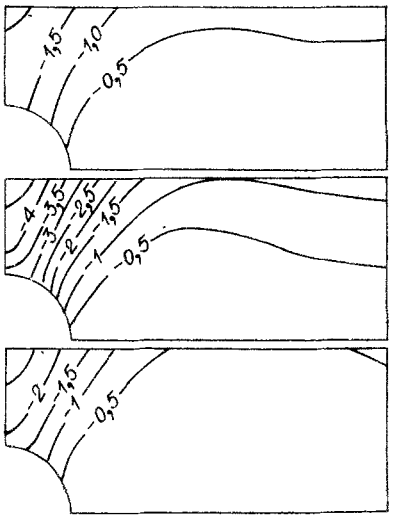

Fig. 7

The stress concentration at the edge of the orifice decreases due to creep. Figure 3 shows the change with time τ of the stress concentration coefficient K, equal to the dimensionless magnitude of the peripheral stress $K = \sigma_\theta = \sigma_{11}$ on the edge of the orifice at the point with coordinates (0, R). The quantity K decreases from $K = 3.7501$ at $\tau = 0$ at $K = 2.5949$ at $\tau = T$. In [1], for an infinitely long plate ($L \to \infty$) the value $K = 3.74$ was given. The coefficient K is independent of P, a, E.

Figure 4 shows the distribution of stress σ_{11} in the plate section $x_1 = 0$, while Fig. 5 is the distribution of peripheral stress $\eta = 1 - 2\theta/\pi$ [θ is the angle in the polar coordinate system (r, θ), see Fig. 1] at times $\tau = 0$ (solid lines) and $\tau = T$ before and after unloading (dashes and dash-dot curves, respectively). The curves are drawn through stress values at the central nodes on the sides of the elements, small stress discontinuities at bounded points between elements are smoothed (in the finite element formulation stress continuity conditions on the boundaries between elements are satisfied only integrally). In the area outside a certain vicinity of the orifice edge the stresses change only insignificantly during the creep process.

Figure 6 shows isolines of axial displacements $u_1 = 1, 2, \ldots$, while Fig. 7 shows transverse stresses $u_2 = -0.5, -1, -1.5, \ldots$ of the Moire pattern type [11, 12] from top to bottom for three states: $\tau = 0$, and $\tau = T$ before and after unloading. The isolines indicate the value of the stress components which are constant thereon.

LITERATURE CITED

1. G. N. Savin, Stress Distribution about Orifices [in Russian], Naukova Dumka, Kiev (1968).
2. Yu. N. Rabotnov, Creep in Construction Elements [in Russian], Nauka, Moscow (1966).

3. R. K. Penny and D. R. Hayhurst, "The deformations and stresses in a stretched thin plate containing a hole during stress redistribution caused by creep," Int. J. Mech. Sci., 11, No. 1 (1969).
4. K. M. Manukyan, V. M. Morozov, and V. T. Sapunov, "Calculating creep in construction elements by the finite element method," Prikl. Mekh., 20, No. 11 (1984).
5. Yu. N. Shevchenko and V. N. Mazur, "Solution of planar and axisymmetric boundary problems of thermoviscoplasticity with consideration of material degradation from creep," Prikl. Mekh., 22, No. 5 (1986).
6. D. R. Hayhurst, P. R. Dimmer, and M. W. Chernuka, "Estimates of the creep rupture lifetime of structures using the finite element method," J. Mech. Phys. Solids, 23, No. 4/5 (1975).
7. G. S. Lee and L. C. Smith, "Analysis of a power-law material containing a single hole subjected to a uniaxial tensile stress using the complex pseudo-stress function," Trans. ASME: J. Appl. Mech., 55, No. 2 (1988).
8. J. Boyle and J. Spence, Stress Analysis in Structures with Creep [Russian translation], Mir, Moscow (1986).
9. K. Yu. Bate and E. L. Wilson, Numerical Analysis Methods and the Finite ELement Method [in Russian], Stroiizdat, Moscow (1982).
10. D. K. Fadeeev and V. N. Fadeeva, Linear Algebra Calculation Methods [in Russian], Fizmatgiz, Leningrad–Moscow (1963).
11. A. Durelli and V. Parks, Moire Analysis of Strain, Prentice-Hall, NJ (1971).
12. V. A. Zhilkin and A. M. Popov, "Study of elastoplastic deformations," Zavod. Lab., 53, No. 9 (1987).

FRACTURE FAILURE IN THE ALLOY AMg6

S. A. Novikov and A. I. Ruzanov

UDC 539.4

Fracture failure in construction materials is preceded by stages of generation, growth, and merger of microcracks of micropores. Studies of the kinetics of fracture formation under dynamic loading resulting from an intense blow on the specimen or its rapid heating have been given a great deal of attention by theoreticians and experimenters. It is well known that the character of failure and the value of fracture strength depend significantly on loading conditions, and the original state of the material. As a rule, generation of microfissures occurs in regions where microstructural defects are located. A promising direction in the study of dynamic failure processes is numerical computer experiment, performed using results of physical experiments. With a proper choice of failure model which considers the real process of fracture formation, such studies permit more detailed clarification of the features of failure.

The present study will offer results of studies in the above direction regarding fracture failure of the aluminum alloy AMg6. This alloy is one of the most widely used materials in modern technology designs, including those used under conditions of intense dynamic loading at elevated temperature. A number of studies have considered its strength characteristics under shock wave loading experimentally (see [1-3] and bibliography therein). In the experiments, results of which were used in the present study for numerical modeling of the fracture failure process, the specimens (80 mm diameter disks 10 mm thick) were loaded by impact of an aluminum plate 4 mm thick, driven to a specified velocity by a sheet charge of explosive material. A portion of the specimens studied were used as supplied (rolled), while a portion were annealed at 320°C for 1 h. Specimens were heated before loading with a radiant heater. After loading, sections were cut from the specimens for metallographic analysis at a magnification of 1000 times. Typical photographs of AMg6 specimen microstructure in the failure generation zone are shown in Fig. 1 (a, temperture 0°C, b, 550°C). Over the entire temperature range generation of microfissures occurred at accumulations of inclusions extended in the direction of rolling. At elevated temperatures merging of the cavities formed occurred primarily in a direction perpendicular to the rolling direction. Cracking along

Moscow. Translated from Zhurnal Prikladnoi Mekhaniki i Tekhnicheskoi Fiziki, No. 2, pp. 158-162, March-April, 1991. Original article submitted March 7, 1989; revision submitted October 10, 1989.

 0021-8944/91/3202-0288$12.50